UTCCP-P-28
Oct. 1997

Hadron spectroscopy and static quark potential in full QCD: A comparison of improved actions on the CP-PACS*

CP-PACS Collaboration:
S. Aoki[a], G. Boyd[b], R. Burkhalter[b], S. Hashimoto[c], N. Ishizuka[a,b], Y. Iwasaki[a,b], K. Kanaya[a,b], T. Kaneko[a], Y. Kuramashi[d], M. Okawa[d], A. Ukawa[a] and T. Yoshié[a,b]

[a]Institute of Physics, University of Tsukuba, Tsukuba, Ibaraki 305, Japan

[b]Center for Computational Physics, University of Tsukuba, Tsukuba, Ibaraki 305, Japan

[c]Computing Research Center, High Energy Accelerator Research Organization (KEK), Tsukuba, Ibaraki 305, Japan

[d]Institute of Particle and Nuclear Studies, High Energy Accelerator Research Organization (KEK), Tsukuba, Ibaraki 305, Japan

We present first results from a full QCD calculation on the CP-PACS, comparing various actions at $a^{-1} \sim 1$GeV and $m_\pi/m_\rho \approx 0.7$–0.9. We use the plaquette and a renormalization group improved action for the gluons, and the Wilson and the SW-Clover action for quarks. We find that significant improvements in the hadron spectrum results from improving the quarks, while the gluon improvement is required for a rotationally invariant static potential. An ongoing effort towards exploring the chiral limit in full QCD is described.

1. Introduction

With the progress in recent years of quenched simulations of QCD, deviations of the quenched hadron spectrum from experiment are becoming apparent. Most recently the precision quenched results from the CP-PACS show a systematic deviation not only in the meson sector, but also in the spectrum of baryons[1]. Clearly the time has come to bolster efforts towards simulations of full QCD.

Full QCD simulations are, however, extremely computer time consuming compared to those of quenched QCD. This leads us to consider improved actions for our simulation of full QCD.

Studies of improved actions have been widely pursued in the last few years. However, a systematic investigation of how various terms added to the gauge and quark actions, taken separately, affect light hadron observables has not been made in full QCD. In this article we report results of such a study carried out on the CP-PACS.

*Talks presented by R. Burkhalter and T. Kaneko at Lattice97, Edinburgh, Scotland, 22–26 July 1997.

2. Actions and simulation parameters

We are carrying out a comparative study of the light hadron spectrum and static quark potential for four action combinations. For gluons we choose either the standard plaquette action (**P**) or an action (**R**) which was obtained by a renormalization group treatment [2] and includes a rectangular Wilson loop. For the quarks we use either the Wilson action (**W**) or the Clover action (**C**) [3]. For the clover coefficient c_{SW} we compare:
(a) the tree value $c_{SW} = 1$.
(b) the meanfield (MF) improved value [4] $c_{SW} = P^{-3/4}$ with P the self-consistently determined plaquette average, and hence a different value of c_{SW} for each K.
(c) a perturbative meanfield (pMF) improved value $c_{SW} = (1 - 0.8412 \cdot \beta^{-1})^{-3/4}$, employed for the **R** action, where the one-loop value is used for the plaquette.
We expect the extent of improvement to be clearer at a coarser lattice spacing. We therefore attempt to tune the coupling constant β so

Table 1
Simulation parameters. All the runs are on a $12^3 \times 32$ lattice, except (*), which is on a $16^3 \times 32$ lattice. For runs marked with (†) the static quark potential is measured. Errors in the mass ratios are statistical but for a^{-1} they are systematic, taking into account uncertainties from the chiral extrapolation.

	β	K	c_{SW}	# conf	m_π/m_ρ	a^{-1} GeV
PW	4.8	.1846		222	.829(1)	
		.1874		200	.772(2)	
		.1891		200	.703(3)	0.99(1)
	5.0†	.1779		300	.846(1)	
		.1798		301	.794(2)	
		.1811		301	.715(4)	1.13(5)
RW	1.9	.1632		200	.899(1)	
		.1688†		200	.803(3)	
		.1713		200	.689(4)	1.22(8)
	2.0†	.1583		300	.898(1)	
		.1623		300	.828(2)	
		.1644		305	.739(3)	1.36(8)

that the lattice spacing equals $a^{-1} \sim 1$GeV.

Our simulations are carried out for two flavors of quarks, mostly on a $12^3 \times 32$ lattice. We employ the hybrid Monte Carlo algorithm to generate full QCD configurations, generally at three values of K corresponding to $m_\pi/m_\rho \approx 0.7$-0.9. Details of the simulation parameters are given in Table 1. For the inversion of the fermion matrix we first used the MR algorithm but switched later to BiCGStab. The molecular dynamics step size is chosen to yield an acceptance of 70-90%.

We measure hadron propagators every 5 trajectories, using smeared sources and point sinks following the method of our quenched study [1]. Errors of masses are determined with a jackknife analysis using a bin size of 5. The lattice spacing is fixed by the ρ meson mass extrapolated to the chiral limit through the form $m_\rho = m_\rho^{(0)} + c_2 m_\pi^2$ or $m_\rho^{(0)} + c_2 m_\pi^2 + c_3 m_\pi^3$. The errors for a^{-1} quoted in Table 1 include the systematic errors in the extrapolation, estimated from the two fitting functions above, and by varying the fitting ranges.

Measurements of the static quark potential are performed on about 100 configurations at those

Table 1
Continued.

PC	5.0	.1590	1.0	100	.826(2)	
		.1610	1.0	100	.791(4)	
		.1630	1.0	101	.712(6)	0.91(2)
	5.0†	.1415	1.855	200	.810(3)	
		.1441	1.825	200	.757(4)	
		.1455	1.805	200	.714(4)	0.88(6)
	5.2†	.1390	1.69	248	.840(2)	
		.1410	1.655	232	.794(3)	
		.1420	1.64	200	.724(8)	1.40(15)
	5.25	.1390	1.637	198	.835(3)	
		.1410	1.61	194	.758(6)	1.5(1)
RC	1.9*	.1370	1.55	203	.845(1)	
		.1400	1.55	198	.779(2)	
		.1420†	1.55	202	.690(3)	
		.1430†	1.55	212	.611(4)	
		.1435	1.55	263	.544(5)	
		.1440	1.55	79	.41(1)	1.19(6)
	1.9†	.1370	1.55	267	.846(2)	
		.1400	1.55	214	.776(2)	
		.1420	1.55	268	.684(3)	0.97(10)
	2.0	.1420	1.0	100	.878(1)	
		.1450	1.0	100	.830(2)	
		.1480	1.0	100	.710(6)	1.24(9)
	2.0	.1300	1.505	100	.910(1)	
		.1370	1.505	90	.794(3)	
		.1388	1.505	90	.710(8)	1.35(20)
	2.0†	.1300	1.54	201	.902(1)	
		.1340	1.529	200	.862(2)	
		.1370	1.52	200	.791(3)	
		.1388	1.515	200	.700(6)	1.35(15)

parameters marked with a † in Table 1. In these measurements we employ the smearing procedure proposed in Ref. [5] and extract the ground state potential in the same way as in Ref. [6].

3. Light hadron spectrum

Our main results for the effect of improved actions on hadron masses are displayed in Fig. 1, in which the ratio m_N/m_ρ is plotted as a function of $(m_\pi/m_\rho)^2$ for the four action combinations. The solid curve represents the well-known phenomenological mass formula [7].

For the standard action combination **PW** (upward triangles), the ratios are well above the

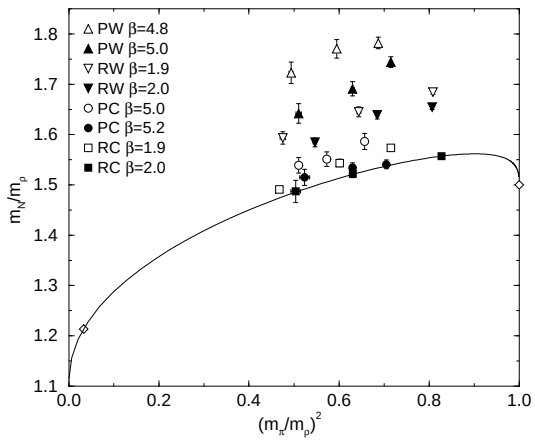

Figure 1. m_N/m_ρ as a function of $(m_\pi/m_\rho)^2$ for four combinations of the action. Clover results are for the choice $c_{SW} = \mathrm{MF}$.

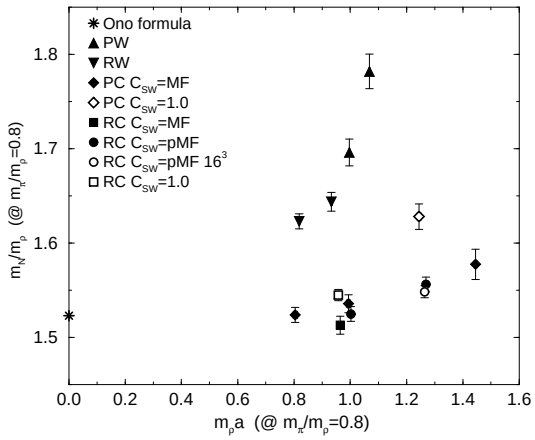

Figure 2. Scaling behaviour of m_N/m_ρ at fixed m_π/m_ρ as a function of $m_\rho a$ for various combinations of the action. The star on the left is the prediction of the phenomenological formula.

phenomenological curve. When we improve the gauge action (the **RW** case, shown by downward triangles), the data points come closer to the curve. By far the most conspicuous change, however, is observed when we introduce the clover term to the quark action. For both the **PC** (circles) and **RC** (squares) cases, the data points lie much nearer to, or on top of, the phenomenological curve.

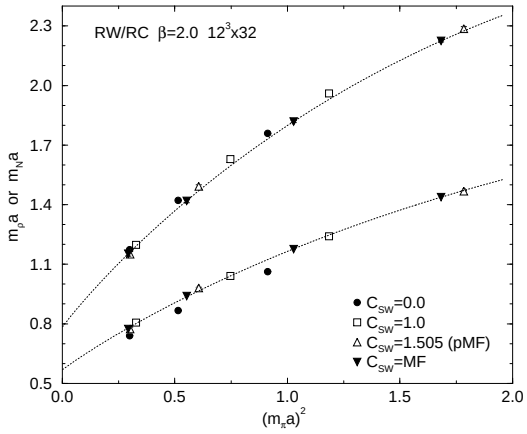

Figure 3. m_ρ and m_N as a function of m_π^2 for different choices of c_{SW}. Dashed lines are chiral fits, cubic in m_π, to data with $c_{SW} = \mathrm{MF}$.

Looking only at Fig. 1, however, is misleading because the runs for different action combinations are performed at slightly different lattice spacings. In Fig. 2 we therefore show the a-dependence. We interpolate the ratios m_N/m_ρ to a common, fixed ratio $m_\pi/m_\rho = 0.8$ and plot m_N/m_ρ vs. m_ρ in lattice units, with m_ρ also interpolated to $m_\pi/m_\rho = 0.8$. Now it becomes clear that the better results for the **RW** case are only due to a finer lattice spacing and that the **PW** and **RW** results seem to lie almost on the same curve. The results for the **PC** and **RC** cases with the MF or pMF choice of c_{SW} also lie on a common curve, which, however, is much flatter. Somewhat less, but still quite substantial, improvement is found for the tree level c_{SW}. The same trend is seen also at $m_\pi/m_\rho = 0.7$ and for the ratio m_Δ/m_ρ [8].

Changing the gluon and quark actions one at a time, we have been able to see clearly that the clover term plays a decisive role in improving the spectrum. In this regard, improving the gluon action has much less effect.

Another interesting feature in our hadron mass data is that they exhibit a negative curvature in terms of m_π^2 towards the chiral limit. In Fig. 3 we show this effect for the ρ meson and nucleon masses using the **RW** and **RC** action combina-

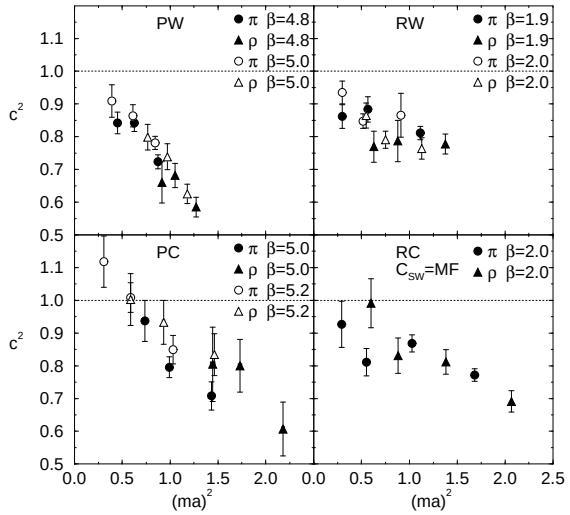

Figure 4. "Speed of light" as a function of the meson mass for four action combinations. Clover results are for the choice $c_{SW} = \mathrm{MF}$

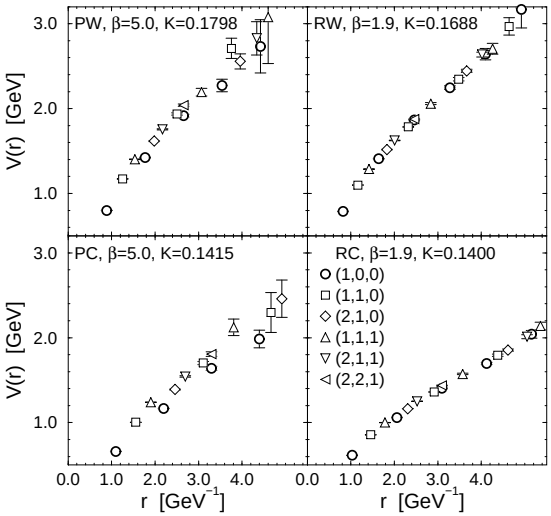

Figure 5. Static quark potential for four action combinations at $m_\pi/m_\rho \simeq 0.8$. Scales are normalized by the lattice spacing determined from m_ρ in the chiral limit. Different symbols correspond to potential data measured in different spatial directions along the vector indicated in the figure. Clover results are for the choice $c_{SW} = \mathrm{MF}$

tions and several choices of c_{SW}. We also note that for the Clover action the ρ meson masses are shifted to a higher value compared to those for the Wilson action. For the nucleon, however, we see no difference between the Wilson and Clover cases. This confirms an earlier observation using staggered dynamical fermions[9].

4. Dispersion relation

Improving the action is expected to lead to a dispersion relation closer to that in the continuum. As a measure for the closeness to the continuum we define the "speed of light" c through $c^2 = dE(p)^2/dp^2|_{p=0}$. Values of c are extracted by a linear fit of $E(p)^2$ to p^2, using the three lowest momenta. In the continuum c equals one for all values of the rest mass. On the lattice, however, c is only expected to go to one for vanishing rest mass. For nonzero rest mass it is generally different from one. An improved action is expected to have a "speed of light" closer to one for nonzero rest masses.

Our results for c are plotted in Fig. 4. An improvement is most clearly seen in a comparison of the **PW** and **RC** action combinations. We are not able to tell whether the improvement is due more to the gauge or quark action, however, since the **RW** and **PC** cases both also show signs of similar improved behavior within the present statistics.

5. Static quark potential

5.1. Rotational symmetry

The static quark potential provides a good measure of the effectiveness of improving the action in restoring the rotational symmetry. In the quenched case it is known that the symmetry is well restored by improving the gauge action[6,10]. Our typical results for full QCD taken for a quark mass corresponding to $m_\pi/m_\rho \approx 0.8$ are plotted in Fig. 5 for each action combination.

We see quite clearly in Fig. 5 that the symmetry is remarkably well restored by improving only the gauge action also in full QCD. The effect of quark action improvement on the restoration of the symmetry is not clear in our data.

This may be explained by the fact that the

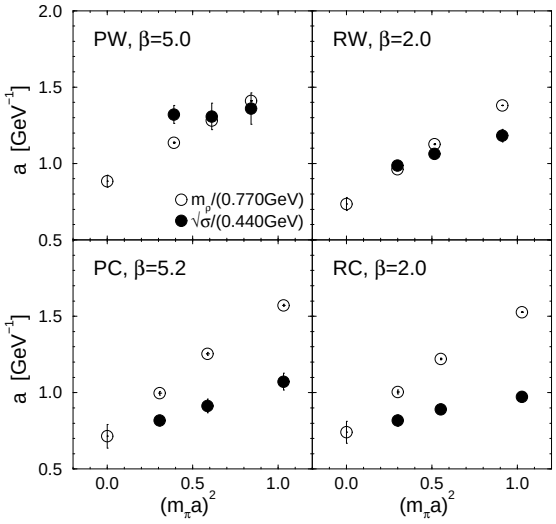

Figure 6. Lattice spacing a determined by the string tension σ and the ρ meson mass as a function of $(m_\pi a)^2$ for the four action combinations. Clover data are for the choice c_{SW} = MF. Filled circles are obtained by identifying $\sigma a^2 = (440\text{MeV})^2$, and open circles from $m_\rho a = 770\text{MeV}$ at each values of K and in the chiral limit.

clover improvement does not remove terms of the Wilson action breaking rotational symmetry, while the **R** action for gluons has much reduced coefficients for the rotationally variant terms compared to the plaquette action.

5.2. Matching of lattice scale

Another interesting question one can address with data for the static potential is whether the lattice scale determined from the string tension σ is consistent with that from the ρ meson mass.

We extract the string tension assuming the form $V(r) = V_0 - \alpha/r + \sigma\cdot r$. The Coulomb coefficient α is ill-determined with our data, which starts at a coarse distance of $r_{\min} = a \approx 0.2$ fm. We therefore fix $\alpha = 0.3$, where χ^2/dof is generally the smallest, and use the shift of σ over the range $\alpha = 0.2 - 0.4$ as a systematic error. This fitting is repeated over several fitting ranges, and the average of the fitted results is taken as the central value of σ, while the variance is included into the systematic error. For estimating

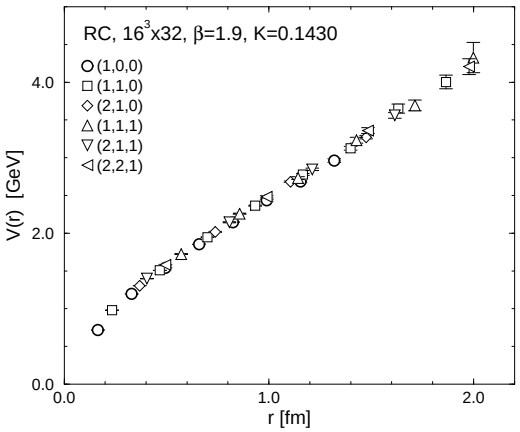

Figure 7. Static quark potential obtained with **RC** action with c_{SW} = pMF on an $16^3\times32$ lattice.

the lattice spacing we employ the phenomenological value $\sigma = (440\text{MeV})^2$. In Fig. 6 we plot the lattice spacing obtained from the string tension and the ρ meson mass for each value of K for all four action combinations. For the ρ meson mass the value in the chiral limit is also shown.

Let us emphasize that the consistency of the two determinations of the lattice scale is expected only in the chiral limit and sufficiently close to the continuum limit. From this point of view, a significant discrepancy in the chiral limit between the two determinations, as observed in the **PW** and **RW** results, shows the presence of large scaling violating effects, originating from the Wilson quark action, at $a^{-1} \approx 1$ GeV. We expect the discrepancy to disappear closer to the continuum limit, and this is supported by the results obtained at $\beta = 5.5$ with $a^{-1} \approx 2$ GeV of Ref. [11].

In contrast, the two estimates of the lattice spacing converge well to a consistent result for the **PC** and **RC** cases. This shows that the clover term helps to improve the consistency of the two determinations of the lattice spacing already at $a^{-1} \approx 1.0$GeV.

5.3. Sea quark effects in the potential

Our results for the potential, plotted in Fig. 5, and covering distances up to $r \approx 1$ fm, are quite linear in r and do not show any sign of string

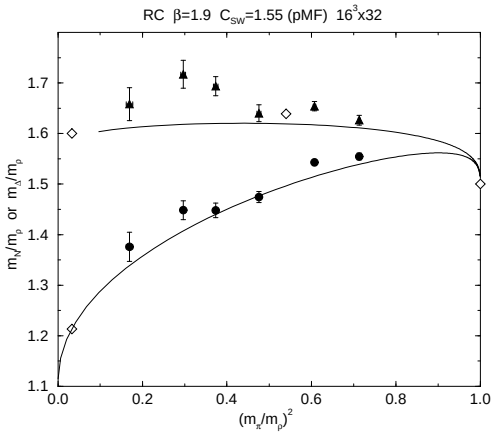

Figure 8. Results on a $16^3 \times 32$ lattice for **RC** action at $\beta = 1.9$. Diamonds are experimental points corresponding to N(940)/ρ(770), Δ(1232)/ρ(770) and Ω(1672)/ϕ(1020).

breaking via $q\overline{q}$ pair creation. In order to search for this effect, we employ one of the **RC** runs carried out on a $16^3 \times 32$ lattice at $\beta = 1.9$ with which we can measure the potential up to $r \simeq$ 2fm. The results are shown in Fig. 7, and still do not show any sign of deviation from a linear behaviour in r.

We find, however, that the maximum overlap of the ground state with the smeared Wilson loop operator decreases as r increases and falls down to about 50% at $r \simeq 2.0$ fm for our full QCD case, while effectively a 100% overlap is obtained for the quenched case, independent of the distance r. This may be an indication that the ground state develops towards larger r a mixing, absent in quenched QCD, with states containing $q\overline{q}$ pairs.

6. Towards the chiral limit

A very interesting and important issue in simulations in full QCD is how close one can approach the chiral limit. Of the four action combinations we have examined, the **RC** combination exhibits the most improved behaviour with regard to the scaling of mass ratios and the rotational symmetry of the potential. We therefore choose this action combination for a feasibility study towards the chiral limit. The runs are made at $\beta = 1.9$ on a $16^3 \times 32$ lattice with a spatial size of about 2.6 fm, and a quark mass corresponding to m_π/m_ρ as small as ≈ 0.4 is explored (see Table 1). Results for the mass ratios obtained with 80–260 configurations for each quark mass, which includes statistics accumulated after the conference (especially for the lightest quark), are shown in Fig. 8.

These results point towards the possiblity that, by improving both the fermion and the gauge action, continuum results in full QCD at small quark masses are achievable using the presently available computing power.

This work is supported in part by the Grants-in-Aid of Ministry of Education, Science and Culture (Nos. 08NP0101, 08640349, 08640350, 08640404, 08740189, and 08740221). Three of us (GB, RB, and TK) are supported by the Japan Society for the Promotion of Science.

REFERENCES

1. CP-PACS Collaboration, these proceedings
2. Y. Iwasaki, Nucl. Phys. B258 (1985) 141; Univ. of Tsukuba report UTHEP-118 (1983), unpublished.
3. B. Sheikholeslami and R. Wohlert, Nucl. Phys. B259 (1985) 572.
4. G.P. Lepage and P.B. Mackenzie, Phys. Rev. D48 (1993) 2250.
5. G.S. Bali and K. Schilling, Phys. Rev. D46 (1992) 2636.
6. Y. Iwasaki *et al.*, Phys. Rev. D56 (1997) 151.
7. S. Ono, Phys. Rev. D17 (1978) 888.
8. CP-PACS Collaboration, in preparation
9. S. Collins *et al.*, Nucl. Phys. B (Proc. Suppl.) 53 (1997) 880.
10. M. Alford *et al.,* Phys. Lett. B361 (1995) 87.
11. K.M. Bitar *et al.*, Nucl. Phys. (Proc. Suppl.) 53 (1997) 225.